



HAL
open science

Amplification de Terrains avec des caractéristiques implicites 3D

Axel Paris, Eric Galin, Adrien Peytavie, Eric Guérin, J Gain

► **To cite this version:**

Axel Paris, Eric Galin, Adrien Peytavie, Eric Guérin, J Gain. Amplification de Terrains avec des caractéristiques implicites 3D. Journées de l'Association Française d'Informatique Graphique, Nov 2018, Poitier, France. hal-03184694

HAL Id: hal-03184694

<https://hal.science/hal-03184694>

Submitted on 29 Mar 2021

HAL is a multi-disciplinary open access archive for the deposit and dissemination of scientific research documents, whether they are published or not. The documents may come from teaching and research institutions in France or abroad, or from public or private research centers.

L'archive ouverte pluridisciplinaire **HAL**, est destinée au dépôt et à la diffusion de documents scientifiques de niveau recherche, publiés ou non, émanant des établissements d'enseignement et de recherche français ou étrangers, des laboratoires publics ou privés.

Terrain Amplification with Implicit 3D Features

A. Paris¹, E. Galin¹, A. Peytavie¹, E. Guérin¹, J. Gain²

¹Université de Lyon, LIRIS, CNRS, UMR5205, France

²University of Cape Town, South Africa

Résumé

While three-dimensional landforms, such as arches and overhangs, occupy a relatively small proportion of most computer-generated landscapes, they are distinctive and dramatic and have an outsize visual impact. Unfortunately, the dominant heightfield representation of terrain precludes such features, and existing in-memory volumetric structures are too memory intensive to handle larger scenes. In this paper, we present a novel memory-optimized paradigm for representing and generating volumetric terrain based on implicit surfaces. We encode feature shape and terrain geology using construction trees that arrange and combine implicit primitives. The landform primitives themselves are positioned using Poisson sampling, built using open shape grammars guided by stratified erosion and invasion percolation processes, and, finally, queried during polygonization.

Mots clé : Procedural modeling, landscape generation, implicit surfaces

1. Introduction

Truly three-dimensional landscape features are some of the most visually arresting and memorable elements of real terrains. They are formed by different physical processes (including joint fracturing, invasion percolation, and stratified erosion), take a variety of forms (from steep-walled canyons to underground cave complexes), and exhibit different scales (from mineral deposits, such as stalactites, less than a meter in diameter, to sea cliffs stretching for kilometers).

Terrains are usually represented by heightfields, which locate scalar elevation values on a regular grid at a single sampling resolution. Existing methods rely either on procedural generation [HGA*10, GGP*15], erosion simulation [MKM89, CGG*17] or example-based synthesis [ZSTR07, GDGP16, GMM15]. Volumetric approaches [PGMG09, BKRE17] suffer from memory and are limited in scope.

We provide a novel solution to the problem of representing, generating and authoring 3D terrain across a range of scales, achieved through a compact volumetric scene representation. Our approach can be integrated with existing modeling pipelines, captures a wide variety of landform features from underground cave complexes to coastal cliffs, incorporates geomorphological effects, such as stratified erosion and invasion percolation, and provides extensive user control.

2. Overview

This section provides an overview of the implicit construction trees that form the basis for the geology and

implicit terrain models central to our technique, followed by a presentation of the workflow.

Construction tree models Two structures are central to our 3D amplification of terrains : a geology model \mathcal{G} for compactly encoding the stratification characteristics of the bedrock, and a terrain model \mathcal{T} that captures complex concave landforms. Both are variants of hierarchical implicit construction trees with leaves that are implicit primitives and internal nodes that are combining operators, in the spirit of [WGG99]. A depth-first walk of such a tree is equivalent to a function evaluation for a given 3D point in the domain.

In the case of geology, leaves of the construction tree are implicit skeletal primitives that define rock resistance for every point in space. The internal nodes are either binary operators for combining sub-trees or unary operators for reproducing folds and faults using various forms of warping. In effect, the geology tree provides a resistance function, denoted as ρ . For terrain, the leaves are implicit shapes hierarchically combined to create specific geomorphological features (e.g., arches or caves) and ultimately merged with the overall terrain using blending, carving and warping operators. The corresponding terrain field function is denoted as f .

Workflow The stages of our amplification process are depicted in Figure 1. To begin with, we automatically switch representations from a $2\frac{1}{2}$ D heightfield \mathcal{H} , provided as input, to an implicit 3D construction tree \mathcal{T} . In this implicitization step care is taken to ensure the initial surface of \mathcal{T} closely matches \mathcal{H} .

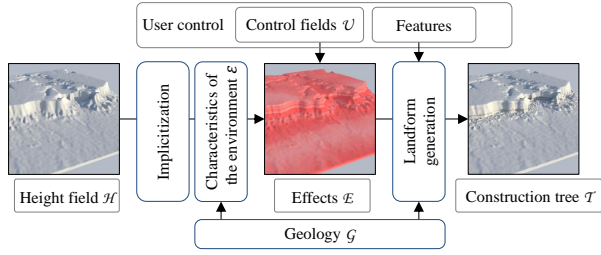


FIGURE 1: Overview of our terrain amplification : Starting from a heightfield \mathcal{H} , we perform an implicitization process to create an implicit representation \mathcal{T} . Using environmental characteristics \mathcal{E} and the underlying geology \mathcal{G} , we apply different forms of augmentation to modify the hierarchical implicit tree structure of the terrain and create 3D features.

This new representation is amenable to various 3D modifications, such as blending and carving. Specifically, we augment \mathcal{T} with 3D landform features synthesized according to the dictates of the environment \mathcal{E} , the underlying geology \mathcal{G} , and the user's requirements. As mentioned, the geology \mathcal{G} expresses the subsurface structure of the terrain, such as strata and fault lines, while the environment represents the agency of wind, sea waves, river flow or rain infiltration. Together they influence the probability of various effects, like erosion events and feature placement. These effects are encoded as sub-trees that are attached to and hence modify the construction tree of the terrain \mathcal{T} . Ultimately, the amplified terrain is polygonized or rendered directly using ray-tracing.

3. Model

Geology Model In our system, the geological characteristics of the terrain \mathcal{G} are defined as a procedural field function $\rho : \mathbb{R}^3 \rightarrow [0, 1]$ that characterizes the strength with which the bedrock resists erosion at any point in space. The softest and hardest bedrock have resistance values of 0 and 1, respectively. Depending on requirements this function may be locally continuous (in the case of folds and warps) or discontinuous (in the case of faults).

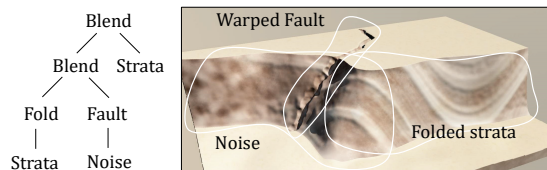


FIGURE 2: Example of the hierarchical construction of a complex geological structure. Horizontal strata (on the right) are folded by warping and a noise function (on the left) is separated off by a fault line.

We implement the resistance function as a hierarchical construction tree (Figure 2), with internal nodes that modify or combine resistance values spatially demarcated by the leaf node primitives. We have created several specific primitives and warping operators to effectively model bedrock strata.

Implicit terrain model Our terrain model \mathcal{T} is based on the same underlying hierarchical construction tree as the geology model. The difference is that primitives and their subtree aggregations portray landform features with a compact volumetric support, such as Hoodoos (Figure 3), rather than strata and rock density. Crucially, the model must also be amenable to the extraction of a final mesh surface. To achieve this, we associate a field function $f : \mathbb{R}^3 \rightarrow \mathbb{R}$ with \mathcal{T} defining the intensity of a given position in space. The surface of the terrain is the set of points where the field function equals a user-defined threshold value T :

$$S = \{\mathbf{p} \in \mathbb{R}^3, f(\mathbf{p}) = T\}.$$

The value of f at a point \mathbf{p} is computed by a depth-first traversal of the construction tree with evaluation of the potential field at each visited node.

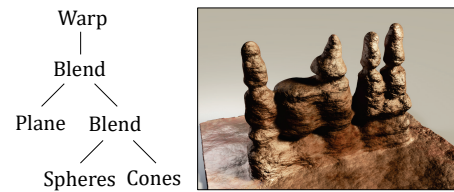


FIGURE 3: In this example the Hoodoos were created by blending several perturbed sphere and cone primitives, and merging with the ground. Creases and cracks were added by a using warping operator.

4. Landform generation

3D landforms are the result of complex erosion processes involving the shape of the terrain, its geology, and the action of environmental erosive agents. Simulating those phenomena would be computationally demanding and prevent interactive control. We thus avoid computationally-intensive physically based simulation and instead, our phenomenological approach augments a $2\frac{1}{2}$ D input terrain with 3D landforms by using controllable and efficient procedural techniques.

4.1. Shallow procedural erosion

Shallow procedural erosion encompasses weathering processes that impact the terrain to a limited depth. Following the general template for landform generation, we proceed in two steps : we first perform Poisson-Sphere sampling in the weathering region to generate a set of points $\{\mathbf{p}_k\}$. Then, at every point \mathbf{p}_k , we locate sphere primitives with a negative energy derived from the weathering intensity at that location $e(\mathbf{p}_k)$.

The effect intensity e at a point is determined by the geology \mathcal{G} , the shape of the terrain \mathcal{H} , and the weathering action. More precisely, we define a parameterized function $e : [0, 1]^2 \rightarrow [0, 1]$ that computes erosion according to the resistance of the rock ρ and the effect stress σ . In our implementation, e is a bi-linear interpolation of these quantities :

$$e(\rho, \sigma) = \sigma(1 - \rho)(1 - \beta) + \sigma\beta$$



FIGURE 4: Various effects achieved with our framework. Sea arches and caves resulting from multiple erosion iterations (left), karst invasion-percolation process on a cliff (center) and a fantastic-scene with floating islands (right).

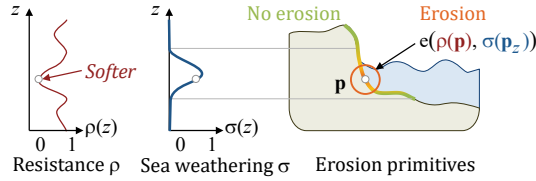


FIGURE 5: Sea erosion impact e combines geology resistance ρ , sea weathering stress σ and accessibility (not illustrated). Sphere primitives are seeded over the surface with a negative energy derived from $e(\rho(\mathbf{p}), \sigma(\mathbf{p}_z))$.

This obeys the constraint that $e(\rho, 0) = 0$, namely that there can be no erosion effect without the rock being under stress. The parameter β controls the erosion intensity for the case where weathering is at a maximum and the material is highly resistant, *i.e.*, $e(1, 1) = \beta$. This accords with the intuition that erosion will be stronger for softer rock under high stress, whereas areas with little stress will not be eroded.

The energy of sphere primitives is proportional to $e(\rho(\mathbf{p}_k), \sigma(\mathbf{p}_k))$. Note that we discard samples with energy below a user-defined threshold, since the associated primitives would have negligible influence.

4.2. Deep procedural erosion

Karst topography leads to caves and sinkholes through the dissolution of soluble rock, such as limestone and gypsum. Below ground they encompass complex drainage systems and networks with underground rivers and caves. On the surface, they are characterized by sinkholes and resurgence points.

We propose an original method for generating karsts, taking our inspiration from *invasion percolation* simulation [WW83]. This is a simplified physical model that simulates the pore-by-pore advancement of a fluid in a porous material when the flow is slow enough that viscosity effects can be neglected. Starting from a set of initial seed points, the algorithm updates a queue \mathcal{Q} of candidates ordered by decreasing material resistance, and progressively advances in the direction of the weakest material, adding new candidates to the queue as the fluid percolates into the material.

First, the queue of candidate points \mathcal{Q} is initialized with the sinkholes of the input terrain. While the queue \mathcal{Q} has candidate points whose resistance is below a user-defined

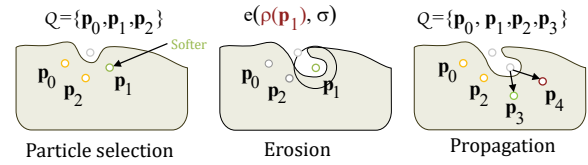


FIGURE 6: Overview of our modified invasion percolation algorithm : after selecting the candidate point with weakest resistance ρ , the terrain is carved by a negative sphere primitive and new candidate points are added to the queue.

threshold, we perform the following steps (Figure 6) : 1) Find the point \mathbf{p}_k in \mathcal{Q} with the least resistance $\rho(\mathbf{p}_k)$ and remove it from \mathcal{Q} ; 2) Locally carve the bedrock by intruding primitives with negative energy into the terrain; 3) Propagate percolation by finding new points in the lower hemisphere at \mathbf{p}_k and add them to \mathcal{Q} .

In the original *invasion percolation* algorithm, step 1) is deterministic, always de-queuing the point with the least resistance. In our implementation, we slightly perturb the resistance by a random factor, whose range ϵ is controlled by the user. We set $\epsilon \approx 0.1$ to allow for more randomness in the selection of candidates, and, consequently, in the shape of the generated networks. The second step carves the terrain only if the rock is sufficiently soft, specifically where $\rho(\mathbf{p}_k) < \rho_0$, with ρ_0 as a user-defined threshold. We modify the energy of the primitive according to the weathering effect, taking into account the stress and rock resistance $e(\rho, \sigma)$ (see Section 4.1). The third step generates new erosion directions. Since we approximate water infiltrating porous stone, we sample a set of random directions on an inverted hemisphere to account for the fact that water flows downwards. New samples are added to the queue \mathcal{Q} only if their Poisson sphere does not intersect other candidates in the queue.

5. Results

We implemented our system in C++. Experiments were performed on a desktop computer equipped with Intel[®] Core i7, clocked at 4GHz with 16GB of RAM, and an NVidia GTX 970 graphics card. The output of our system was streamed into Vue Xstream[®] to produce photo-realistic landscapes (Figure 4).

Control Our method provides several mechanisms for user control over landform generation. First, a user can define the

regions to be amplified with erosion effects or landform features, by either directly painting a control region onto the 2D input terrain or by marking out a spatial volume. Effects can also be fine-tuned by changing their generative parameters. In contrast with most simulation-based methods, these parameters have a direct and intuitive physical interpretation (for example, the height and base radius of the Hoodoos or the maximum depth of sea erosion). Finally, the user can enter an interactive editing session and sculpt the terrain with extruding or intruding skeletal primitives. A key benefit of our framework is that our terrain models offer a single consistent global scene structure. This means that the user can seamlessly switch between authoring and simulation over as many cycles of iterative refinement as required.

Performance Table 1 reports different statistics for several landscapes, namely the extent of the input terrain, the number of primitives produced by the 3D augmentation methods, the ratio between the surface terrain and the surface occupancy of 3D primitives, the amount of memory, the generation time. Our amplification methods generates the construction tree representing complex landform features at a precision of $\approx 10\text{cm}$ in less than 7 seconds for terrains that extend over 5km^2 .

TABLE 1: Statistics for our terrains : size [km^2], number of nodes in the construction tree $\#\mathcal{N}$, relative area percentage of 3D a , generation time [s] and memory footprint [Mb].

Scene	Size	$\#\mathcal{N}$	a	Gen.	Mem.
Sea (4)	6.0	50693	0.01	6.86	3.04
Karst (4)	5.2	165773	0.02	6.52	9.95

Memory Our hierarchical implicit construction tree efficiently models 3D features with a reduced memory overhead. One important aspect of our approach is that implicit primitives are only located where needed. Thus, most of our scenes have a low ratio a compared to their size. Our implicit model and the use of skeletal primitives allows us to represent a high number of local volumetric features with the minimum information in memory.

Control Our system integrates user-control and authoring at the different stages of the pipeline. The fold, faults and different strata of the geology can be controlled easily. The procedural generation algorithms are parameterized with a few intuitive parameters. Finally, the user can directly sculpts landform features by merging the terrain with primitives or even subtrees.

Extensibility Our hierarchical implicit construction tree embeds heightfield representations at an extremely reduced cost, and allows us to augment $2\frac{1}{2}$ D terrains with 3D landforms. An important feature of our model is that it can be extended with new operators, primitives or other algorithms easily.

6. Conclusion

We have introduced a novel method for augmenting $2\frac{1}{2}$ D heightfields with 3D landforms. Such 3D landforms as sea cliffs, canyons with overhangs, network of caves and tunnels, Hoodoos and Goblins, and even floating islands, are essential scenic elements in synthetic environments, animated films and computer games. In future, we would like to investigate the implicit modeling of finely-detailed rock features at scales below 10cm .

Acknowledgments

This work is part of the project *PAPAYA* funded by the *Fonds National pour la Société Numérique* and the project HDW ANR-16-CE33-0001, supported by Agence Nationale de la Recherche. This work also received a grant from Bourg en Bresse city and CCI de l’Ain. We would like to credit E-on software for providing *Vue xStream* for rendering our terrain models.

Références

- [BKRE17] BECHER M., KRONE M., REINA G., ERTL T. : Feature-based volumetric terrain generation. In *Proceedings of the 21st ACM SIGGRAPH Symposium on Interactive 3D Graphics and Games* (2017), I3D ’17, pp. 10 :1–10 :9.
- [CGG*17] CORDONNIER G., GALIN E., GAIN J., BENES B., GUÉRIN E., PEYTAVIE A., CANI M.-P. : Authoring Landscapes by Combining Ecosystem and Terrain Erosion Simulation. *ACM Transactions on Graphics*. Vol. 36, Num. 4 (2017).
- [GDGP16] GUÉRIN E., DIGNE J., GALIN E., PEYTAVIE A. : Sparse representation of terrains for procedural modeling. *Computer Graphics Forum (Proceedings of Eurographics)*. Vol. 35, Num. 2 (2016), 177–187.
- [GGP*15] GÉNEVAUX J.-D., GALIN E., PEYTAVIE A., GUÉRIN E., BRIQUET C., GROSBELLET F., BENES B. : Terrain modeling from feature primitives. *Computer Graphics Forum*. Vol. 34, Num. 6 (2015), 198–210.
- [GMM15] GAIN J. E., MERRY B., MARAIS P. : Parallel, realistic and controllable terrain synthesis. *Computer Graphics Forum*. Vol. 34, Num. 2 (2015), 105–116.
- [HGA*10] HNAIDI H., GUÉRIN É., AKKOUCHE S., PEYTAVIE A., GALIN É. : Feature based terrain generation using diffusion equation. *Computer Graphics Forum*. Vol. 29, Num. 7 (2010), 2179–2186.
- [MKM89] MUSGRAVE F. K., KOLB C. E., MACE R. S. : The synthesis and rendering of eroded fractal terrains. *Computer Graphics*. Vol. 23, Num. 3 (1989), 41–50.
- [PGMG09] PEYTAVIE A., GALIN É., MÉRILLOU S., GROSGEANT J. : Arches : A framework for modeling complex terrains. *Computer Graphics Forum*. Vol. 28, Num. 2 (2009), 457–467.
- [WGG99] WYVILL B., GUY A., GALIN É. : Extending the CSG tree - warping, blending and boolean operations in an implicit surface modeling system. *Computer Graphics Forum*. Vol. 18, Num. 2 (1999), 149–158.
- [WW83] WILKINSON D., WILLEMSSEN J. F. : Invasion percolation : a new form of percolation theory. *Journal of Physics A : Math. Gen.* Vol. 16 (1983).
- [ZSTR07] ZHOU H., SUN J., TURK G., REHG J. M. : Terrain synthesis from digital elevation models. *Transactions on Visualization and Computer Graphics*. Vol. 13, Num. 4 (2007), 834–848.